

# Dynamics of the Ionization Processes of Benzene–H<sub>2</sub>O Clusters: A Direct ab Initio Dynamics Study

Hiroto Tachikawa\* and Manabu Igarashi

Division of Molecular Chemistry, Graduate School of Engineering, Hokkaido University, Sapporo 060-8628, Japan

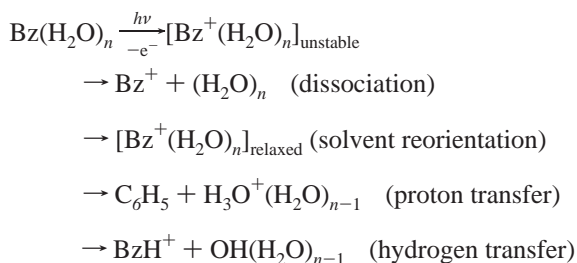
Received: March 11, 1998; In Final Form: June 1, 1998

Ionization processes of benzene–water cluster Bz(H<sub>2</sub>O)<sub>n</sub> (*n* = 1 and 2) have been studied by means of direct ab initio dynamics calculations. The ab initio calculations for the BzH<sub>2</sub>O 1:1 neutral complex show that in the minimum energy structure the water hydrogens point toward the center of mass of the benzene ring (the dipole orientation form). The potential energy curve calculated as a function of the benzene–H<sub>2</sub>O center of mass distance (*R*<sub>cm</sub>) indicates that the H<sub>2</sub>O molecule is weakly bound to the benzene ring. The potential energy curve for the cationic system BzH<sub>2</sub>O<sup>+</sup> constrained to the dipole orientation form is purely repulsive, whereas the curve calculated for the oxygen orientation form has a fairly deep well. The complex has a wide Franck–Condon (FC) region for the ionization. Dynamics of the ionization process of the BzH<sub>2</sub>O complex was studied by means of direct ab initio dynamics calculations. A total of 11 points in the FC region were chosen as initial points. The trajectories started from both the equilibrium point of BzH<sub>2</sub>O (*R*<sub>cm</sub> = 3.395 Å) and the outer classical turning point in the FC region (*R*<sub>cm</sub> = 3.60 Å) gave a strongly bound BzH<sub>2</sub>O<sup>+</sup> complex as a product, whereas the trajectory from the inner classical turning point (*R*<sub>cm</sub> = 2.95 Å) leads to the dissociation product (Bz<sup>+</sup> + H<sub>2</sub>O). The reaction mechanism of the ionization processes of the BzH<sub>2</sub>O complex was discussed on the basis of these theoretical results.

## 1. Introduction

The photoionization of the hydrogen-bonded cluster and complexes plays an important role in gaseous ion chemistry and in interstellar clouds.<sup>1–3</sup> Many such clusters have been investigated both experimentally and theoretically. Benzene is one of the prototype molecules that form  $\pi$ -type hydrogen-bonded complexes with several atoms and molecules such as Ar, HCl, NH<sub>3</sub>, and H<sub>2</sub>O. Benzene–H<sub>2</sub>O clusters, Bz(H<sub>2</sub>O)<sub>n</sub>, have been extensively studied by several groups.<sup>3a</sup> Recently, Courty et al. investigated the ionization of size-selected benzene–water clusters Bz(H<sub>2</sub>O)<sub>n</sub> by means of resonance-enhanced multiphoton ionization.<sup>4</sup> They showed that for medium-sized clusters (*n* = 22–28) a proton may transfer from the benzene cation to one of the associated water molecules. Zwier and co-workers measured resonant two-photon ionization (R2PI) time-of-flight mass spectra of Bz(H<sub>2</sub>O)<sub>n</sub> complexes (*n* = 1 or 2). They found that BzH<sub>2</sub>O<sup>+</sup> complex is formed by the photoionization of the Bz(H<sub>2</sub>O)<sub>n</sub> complex.<sup>3</sup> Thus, clusters composed of water and benzene are typical of hydrogen-bonded clusters as regards to the photoionization dynamics.

The photoionization of the benzene–water cluster may cause mainly five relaxation channels:



The interaction between Bz and H<sub>2</sub>O is suddenly and strongly

changed by photoionization so that a few reaction channels are possibly competitive. The first channel is a loss of H<sub>2</sub>O from the benzene cluster. The second channel involves rearrangement and reorientation of the water molecules in the cluster. The third and fourth channels are transfer of a proton from the benzene cation to a water molecule and abstraction of a hydrogen atom from a water molecule by the cation. It is experimentally known that the third and fourth channels are energetically less favored in small-sized clusters. Hence, only the first two channels are open in the case of photoionization of the BzH<sub>2</sub>O 1:1 complex.

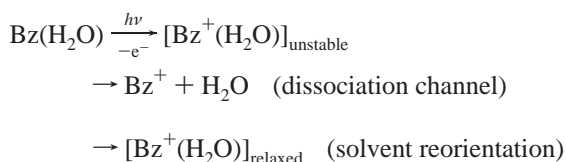
Ab initio MO calculations of BzH<sub>2</sub>O 1:1 neutral complex have been carried out by several groups.<sup>5</sup> Kim et al. calculated the structure of BzH<sub>2</sub>O complex at the MP2/6-311++G(3df,-2pd) level.<sup>5a</sup> These results indicated that the water molecule is weakly bound on the benzene ring by the interaction between the hydrophobic  $\pi$ -electron of Bz and water hydrogens. The most stable structure is one in which the plane of the water molecule is perpendicular to the benzene ring with the water hydrogens pointing toward the ring. Recently, Gregory and Clary<sup>5d</sup> carried out diffusion quantum Monte Carlo simulation to determine the structure of the complex BzH<sub>2</sub>O. Their simulation indicated that the vibrational averaging renders the hydrogens indistinguishable, although the minimum energy structure can be considered to have a single hydrogen bond. The large-amplitude motions of H<sub>2</sub>O present in this complex make it difficult to determine an equilibrium structure at finite temperature.

The BzH<sub>2</sub>O complex has been also investigated experimentally by several groups.<sup>3</sup> Cheng et al. measured the dissociation energy of the BzH<sub>2</sub>O complex by means of the threshold difference method.<sup>6</sup> The dissociation energies obtained for BzH<sub>2</sub>O and BzH<sub>2</sub>O<sup>+</sup> are *D*<sub>0</sub>(BzH<sub>2</sub>O) = 2.25 ± 0.28 kcal/mol and *D*<sub>0</sub>(BzH<sub>2</sub>O<sup>+</sup>) = 4.0 ± 0.4 kcal/mol, respectively. Thus, the previous studies mainly focused on the structures and

\* Author to whom correspondence should be addressed. E-mail: hiroto@eng.hokudai.ac.jp. Fax: +81 11706-7897.

dissociation energies of BzH<sub>2</sub>O and Bz<sup>+</sup>H<sub>2</sub>O. The ionization dynamics of BzH<sub>2</sub>O is scarcely known.

In the present study, direct ab initio dynamics calculations<sup>8</sup> are carried out in order to elucidate the ionization processes of BzH<sub>2</sub>O complex. From the energetics, it can be considered that two reaction channels



would proceed competitively, where [Bz<sup>+</sup>(H<sub>2</sub>O)]<sub>unstable</sub> is an unstable state formed by vertical ionization of neutral complex and [Bz<sup>+</sup>(H<sub>2</sub>O)]<sub>relaxed</sub> is a complex cation of BzH<sub>2</sub>O<sup>+</sup>, which is energetically and structurally relaxed. We focus our attention mainly on preference of the reaction channels after the photoionization of BzH<sub>2</sub>O in the present study. The main purposes of this study are (1) to elucidate qualitatively the ionization dynamics of Bz(H<sub>2</sub>O)<sub>n</sub> (*n* = 0–2) on the basis of the direct ab initio dynamics calculation and (2) to determine the origin of the preference of the reaction channels.

## 2. Computational Methods

Usually, the classical trajectory calculations are performed using an analytically fitted potential energy surface, as we have done previously.<sup>7</sup> However, it is not appropriate to predetermine the reaction surfaces of the present systems because of the large number of degrees of freedom ( $3N - 6 = 39$  where *N* is number of atoms in the system). Therefore, in the present study, we applied the direct ab initio dynamics method with all degrees of freedom. The details of the direct dynamics method are described elsewhere.<sup>8</sup>

In the direct ab initio dynamics calculation, we used the 3-21G basis set for the ionization process of BzH<sub>2</sub>O throughout. First, a trajectory calculation of the neutral system BzH<sub>2</sub>O was carried out in order to obtain the initial structure of BzH<sub>2</sub>O<sup>+</sup>. The HF/3-21G optimized geometry of BzH<sub>2</sub>O was chosen as an initial structure. At the start of the trajectory calculation, atomic velocities are adjusted to give a temperature of 10 K. Temperature was defined by

$$T = \frac{1}{3Nk} \left\langle \sum_{i=1}^N m_i v_i^2 \right\rangle$$

where *N* is number of atoms, *v<sub>i</sub>* and *m<sub>i</sub>* are the velocity and mass of the *i*th atom, and *k* is Boltzmann's constant. The equations of motion for *n* atoms in a molecule are given by

$$\begin{aligned} \frac{dQ_j}{dt} &= \frac{\partial H}{\partial P_j} \\ \frac{\partial P_j}{\partial t} &= - \frac{\partial H}{\partial Q_j} = - \frac{\partial U}{\partial Q_j} \end{aligned}$$

where *j* = 1–3*N*, *H* is the classical Hamiltonian, *Q<sub>j</sub>* is the Cartesian coordinate of the *j*th mode, and *P<sub>j</sub>* is the conjugate momentum. These equations were numerically solved by the Runge–Kutta method. No symmetry restriction was applied to the calculation of the gradients in the Runge–Kutta method. The time step size was chosen as 0.10 fs, and a total of 10 000 steps were calculated for each trajectory. The drift of the total energy was confirmed to be less than 0.1% for an entire

trajectory. It was also confirmed that the momentum of the center of mass and the angular momentum around the center of mass retained their initial values of zero.

In the direct ab initio dynamics calculations for BzH<sub>2</sub>O<sup>+</sup>, the optimized structure of BzH<sub>2</sub>O was first chosen as the initial structure of BzH<sub>2</sub>O<sup>+</sup>. The optimized structure (HF/3-21G) has a distance of 3.3950 Å for the center-of-mass distance between Bz and H<sub>2</sub>O (*R<sub>cm</sub>*). Second, we chose two typical points on the edges of the Franck–Condon (FC) region for the direction of *R<sub>cm</sub>*: inner and outer classical turning points in the FC region. In addition to the three points (the equilibrium, inner, and outer classical turning points), more than eight points were randomly selected from the FC region obtained by the trajectory calculation for the BzH<sub>2</sub>O neutral system. A total of 11 trajectories for the BzH<sub>2</sub>O<sup>+</sup> system were run from the selected points on the FC region. The velocities of the atoms and the excess energy of the system were assumed to be zero at the initial points of the trajectories calculated for BzH<sub>2</sub>O<sup>+</sup>.

To obtain detailed structures and the energetics of the BzH<sub>2</sub>O and Bz<sup>+</sup>H<sub>2</sub>O complexes, ab initio MO calculations<sup>9</sup> were carried out at the HF and MP2 levels of theory with 3-21G and 6-31G\* basis sets.

## 3. Results

**I. Ab Initio MO Calculations. A. Structure of BzH<sub>2</sub>O Neutral Complex.** First, the geometry of the BzH<sub>2</sub>O neutral complex was fully optimized by means of the HF/3-21G, MP2/6-31G\*, and MP2/6-311G(d,p) calculations. In this section, we will discuss the results obtained by the MP2/6-31G\* calculation. The optimized geometrical parameters are summarized in Table 1. The structure of BzH<sub>2</sub>O is schematically illustrated in Figure 1 (upper). In the stable structure of BzH<sub>2</sub>O, the water molecule is situated over the center of mass of the benzene ring (CM) with the following dipole orientation: the hydrogens of H<sub>2</sub>O point toward the benzene ring with one of the hydrogens of H<sub>2</sub>O slightly near the benzene ring. The stable structure has *C<sub>s</sub>* symmetry. The center-of-mass distance between Bz and H<sub>2</sub>O in the BzH<sub>2</sub>O complex (*R<sub>cm</sub>*) and the C···O distance (*r<sub>3</sub>*) were calculated to be 3.244 and 3.532 Å, respectively. The structural features thus obtained are in reasonably agreement with the previous experimental and theoretical findings.<sup>3,5,10–12</sup>

**B. Structures of BzH<sub>2</sub>O<sup>+</sup> Complex.** The most stable structure optimized for the BzH<sub>2</sub>O<sup>+</sup> cation (denoted by complex **I**) is illustrated in Figure 1 (middle). The optimized parameters for complex **I** are given in Table 1. The structure obtained for BzH<sub>2</sub>O<sup>+</sup> is quite different from that of BzH<sub>2</sub>O; the oxygen of the water molecule is in the plane of the benzene plane. It interacts with hydrogens of Bz<sup>+</sup> through a dipole-charge (hole) force. The two hydrogens of Bz<sup>+</sup> interact similarly to the oxygen of H<sub>2</sub>O.

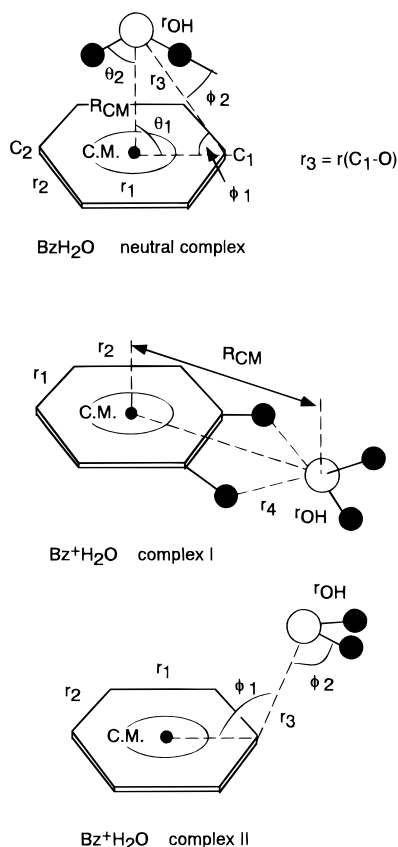
In addition to complex **I**, the geometry optimizations gave another complex (denoted by complex **II**), which is illustrated in Figure 1 (lower). Complex **II** is higher in energy than complex **I**, as will be shown in the next section. In complex **II**, the water oxygens are closest to one carbon atom of the benzene ring. The interaction between H<sub>2</sub>O and the benzene cation (Bz<sup>+</sup>) arises from the mixing of oxygen occupied by two electrons and a π-orbital of a carbon atom occupied by one electron. These orbitals combine to give a σ\* orbital, which is occupied by one electron. In other words, the bonding interaction is a σ\*(π–π) interaction.

**C. Energetics.** Relative energies of the complexes calculated at the several levels of theory are listed in Table 2. Zero level corresponds to the energy of the dissociation limit for the

**TABLE 1: Optimized Structures Calculated at Several Levels (Bond Lengths and Angles Are in Angstroms and Degrees, Respectively)**

	neutral complex <sup>a</sup>			complex I		complex II	
	HF/3-21G	MP2/6-31G*	MP2/6-311G**	HF/3-21G	MP2/6-31G*	HF/3-21	MP2/6-31G*
$R_{\text{cm}}$	3.395	3.244	3.174	4.047	4.167	2.625	3.673
$r_{\text{OH}}$	0.966	0.969	0.959	0.968	0.971	.972	0.971
$r_1$	1.386	1.398	1.400	1.449	1.453	1.474	1.460
$r_2$	1.385	1.397	1.399	1.378	1.385	1.370	1.392
$r_3$	3.667	3.532	3.469	2.949	3.063	1.723	2.878
$r_4$				2.243	2.347		
$\theta_1$	90.1	90.1	90.2				
$\theta_2$	53.2	51.1	50.3				
$\phi_1$	67.7	66.6	66.1			111.9	114.7

<sup>a</sup> MP2/6-31+G\* and MP2/6-311++G(2d,p) values of  $R_{\text{cm}}$  (ref 5a) are 3.420 and 3.310 Å, respectively.

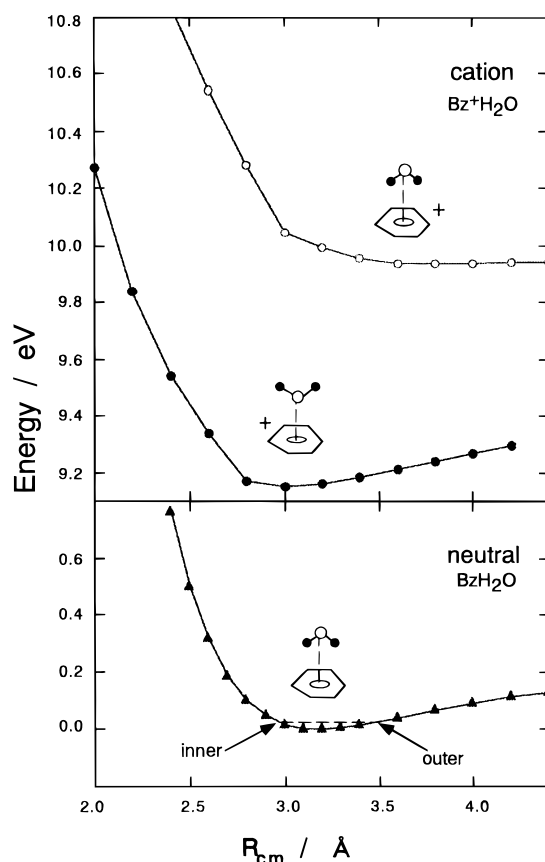
**Figure 1.** Structures and geometrical parameters of benzene–water complex ( $\text{BzH}_2\text{O}$ ) and its cation complexes (complexes I and II).**TABLE 2: Relative Energies (in eV)**

	HF/3-21G//HF/3-21G	HF/6-31G*//HF/6-31G*	MP2/6-31G*//MP2/6-31G*
$\text{Bz}^+ + \text{H}_2\text{O}$	0.0	0.0	0.0
<b>I</b>	-0.81	-0.50	-0.57
<b>II</b>	-0.78	-0.36	-0.40
$\text{BzH}_2\text{O}^a$	-8.09	-7.73	-9.00

<sup>a</sup> Experimental value is -9.246 eV (ref 6).

cationic system ( $\text{Bz}^+ + \text{H}_2\text{O}$ ). All calculations show a similar tendency for the energetics of  $\text{BzH}_2\text{O}^+$  system. Both complexes I and II have negative energy, suggesting that the complexes are energetically more stable than the dissociation limit for the cationic system ( $\text{Bz}^+ + \text{H}_2\text{O}$ ). All calculations indicate that complex I is energetically favored for  $\text{BzH}_2\text{O}^+$  system. At the MP2/6-31G(d,p) level of theory, the energy of complex I is 0.17 eV lower than that of complex II.

Total energies for the neutral system were also calculated at the same levels. The energy of the  $\text{BzH}_2\text{O}$  complex is ca. 8–9

**Figure 2.** Potential energy curves calculated as a function of  $R_{\text{cm}}$  at the MP2/6-311G(d,p) level. Upper and lower panels are PECs for neutral and cationic systems of  $\text{BzH}_2\text{O}$ , respectively. Lower PEC in the upper panel is calculated by using the oxygen orientation form (see text).

eV lower than the dissociation limit for the cationic system. It should be noted that the results of the HF/3-21G method give qualitatively reasonable energies in the  $\text{BzH}_2\text{O}^+$  system.

**D. Potential Energy Curves.** The potential energy curve (PEC) calculated as a function of  $R_{\text{cm}}$  distance for the  $\text{BzH}_2\text{O}$  neutral system is given in Figure 2 (lower panel). The values were calculated at the MP2/6-311G(d,p) level. The geometrical parameters except for  $R_{\text{cm}}$  are fixed at those optimized for  $\text{BzH}_2\text{O}$  (i.e., the dipole orientation form). The PEC shows that  $\text{H}_2\text{O}$  is bound on the benzene ring and that the potential minimum is located at  $R_{\text{cm}} = 3.20$  Å. The shape of the PES around the minimum point is very flat along the  $R_{\text{cm}}$  direction. The binding energy of  $\text{H}_2\text{O}$  to the benzene ring was calculated to be 3.0 kcal/mol at the MP2/6-311G(d,p) level. These results indicate that the  $\text{H}_2\text{O}$  molecule is weakly bound to the benzene

ring in the neutral complex and that the structure of this complex is not at all rigid.

For the cationic system BzH<sub>2</sub>O<sup>+</sup>, first, the PEC was calculated at the UMP2/6-311G(d,p) level (upper curve in upper panel). The geometrical parameters used in the PEC calculation are the same as those for the neutral state; i.e., they retain dipole orientation form. The shape of PEC for BzH<sub>2</sub>O<sup>+</sup> is much different from that of neutral state; the PEC for the cationic system is repulsive, although a shallow minimum is found at  $R_{\text{cm}} = 3.60$  Å. However, its binding energy is negligibly small.

Second, the PEC for the complex cation BzH<sub>2</sub>O<sup>+</sup> in which the oxygen atom orients toward the benzene ring (the oxygen orientation form is Bz<sup>+</sup>⋯OH<sub>2</sub>) was calculated. The same geometrical parameters as those for BzH<sub>2</sub>O were used for Bz<sup>+</sup> and H<sub>2</sub>O in the PEC calculation. The result is plotted in Figure 2 (lower curve in upper panel). The energy for the oxygen orientation form (Bz<sup>+</sup>⋯OH<sub>2</sub>) is considerably lower, and the PEC has an attractive part. The energy for the minimum point ( $R_{\text{cm}} = 3.0$  Å) is 9.15 eV higher than that of BzH<sub>2</sub>O. The equilibrium distance of  $R_{\text{cm}}$  for Bz<sup>+</sup>⋯OH<sub>2</sub> ( $R_{\text{cm}} = 3.0$  Å) is slightly shorter than that for the BzH<sub>2</sub>O neutral complex (3.20 Å). It should be noted that the FC region for ionization of BzH<sub>2</sub>O is significantly wide because of the fact that the potential is very shallow at the ground state. Hence, it is expected that the ionization from the wide FC region will occur.

The similar calculations of PECs were carried out at the HF/3-21G level. Although the equilibrium bond length of Bz(H<sub>2</sub>O) calculated by HF/3-21G ( $R_{\text{cm}}$ ) is slightly longer than that by MP2/6-311G(d,p) calculation ( $R_{\text{cm}} = 3.39$  vs 3.20 Å), the shapes of PECs obtained are quite close to those calculated at the MP2/6-311G(d,p) level. The experimental values for  $R_{\text{cm}}$  have been reported to be  $3.32 \pm 0.07$ ,<sup>10</sup> 3.329,<sup>11</sup> and  $3.347 \pm 0.005$  Å,<sup>12</sup> suggesting that the HF/3-21G calculation would give a reasonable structure of BzH<sub>2</sub>O and reasonable results for the dynamics. Therefore, we use the HF/3-21G level of theory in the following dynamics calculation.

**II. Ab Initio Dynamics Trajectory Study.** *A. Structure of Neutral BzH<sub>2</sub>O.* The ab initio MO calculations showed that the BzH<sub>2</sub>O is a floppy complex in which H<sub>2</sub>O is weakly bonded to the benzene ring with its C<sub>2</sub> axis coincident with the C<sub>6</sub> axis of the ring. Hence, the vibrational amplitude of H<sub>2</sub>O along the  $R_{\text{cm}}$  direction is large at finite temperature. To obtain the structure of BzH<sub>2</sub>O at finite temperature, a trajectory for the BzH<sub>2</sub>O neutral complex was calculated at constant temperature. We chose 10 K for a simulation temperature and 0.01 ps for a bath relaxation time. The optimized structure of BzH<sub>2</sub>O was chosen as the initial structure. The energy of the system calculated as a function of time was close to a constant value during simulation (figure is not given). The profile of the trajectory at 10 K is given in Figure 3. The center-of-mass distance ( $R_{\text{cm}}$ ) and two bond distances,  $r(\text{C}_1\text{--C}_2)$  in benzene ring and  $r_3 = r(\text{C}_1\text{--O})$ , are plotted in Figure 3A as a function of simulation time. The center-of-mass distance oscillates slowly around the equilibrium point and the position of oxygen measured from a carbon atom,  $r_3 = r(\text{C}_1\text{--O})$ , oscillates with a similar vibration period. The C-C bond distance in benzene,  $r_1 = r(\text{C--C})$ , oscillated rapidly within 2.75–2.78 Å. The O-C<sub>1</sub>-CM angle ( $\phi_1$ ) oscillated slowly in the neutral system as clearly seen in Figure 3B. These results indicate that the BzH<sub>2</sub>O has a very nonrigid structure even at low temperature and that it has a wide Franck-Condon (FC) region for the ionization.

*B. Ionization Process in BzH<sub>2</sub>O.* To describe the dynamics of BzH<sub>2</sub>O<sup>+</sup> following the ionization, direct ab initio dynamics

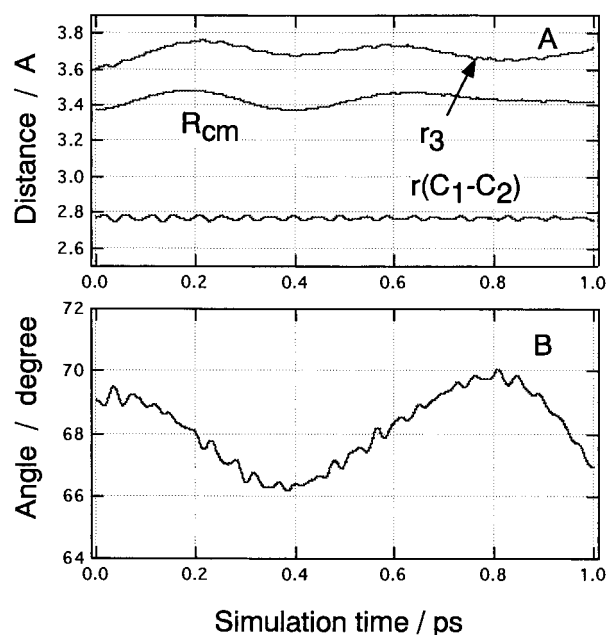


**Figure 3.** Trajectory for the neutral BzH<sub>2</sub>O complex plotted as a function of reaction time: (A) interatomic distances  $R_{\text{cm}}$ ,  $r(\text{C}_1\text{--C}_2)$ , and  $r_3$  vs time; (B) angle of O-C<sub>1</sub>-C<sub>CM</sub> ( $\phi_1$ ) vs time. The simulation is carried out at 10 K.

calculations were carried out. Vertical ionization of BzH<sub>2</sub>O was assumed. As suggested in the previous section, the FC region for ionization is rather large. Hence, we chose several points on the FC region as the initial geometry in the dynamics calculations. A total of 11 trajectories were run from the selected points. First, we chose the optimized structure of BzH<sub>2</sub>O as the initial structure: the equilibrium point of the BzH<sub>2</sub>O complex ( $R_{\text{cm}} = 3.395$  Å). Next, the classical turning points of FC region for the  $R_{\text{cm}}$  direction were chosen:  $R_{\text{cm}} = 2.95$  and 3.60 Å. These are denoted by inner and outer classical turning points, respectively. These distances were estimated from the PEC for the BzH<sub>2</sub>O system (Figure 2) and zero-point vibrational energy for the  $R_{\text{cm}}$  direction ( $91$  cm<sup>-1</sup>). The other eight points were randomly selected from the structures determined by the trajectory calculation of neutral BzH<sub>2</sub>O complex, i.e., FC region (Figure 3). In this section, we discuss the mechanism of the ionization of BzH<sub>2</sub>O using mainly the results of the trajectories started from the former three points.

The computed trajectories lead to two reaction channels: the dissociation and complex channels. In the complex formation channel, both complexes **I** and **II** were formed. However, we do not distinguish complexes **I** and **II** in the trajectory calculation because we are interested in only the reaction channels: dissociation and complex formation.

*Trajectory from the Equilibrium Point of BzH<sub>2</sub>O.* Figure 4 shows the result of trajectory started from  $R_{\text{cm}} = 3.395$  Å (i.e., the equilibrium point). The potential energy (PE) for the trajectory is plotted in Figure 4A as a function of reaction time. The zero level of the PE corresponds to the energy at the starting point on potential energy surface for the cationic system BzH<sub>2</sub>O<sup>+</sup>. At very short time (0–0.02 ps), the energy drops suddenly to  $-3.0$  kcal/mol because of the Jahn-Teller effect in singly ionized benzene (Bz<sup>+</sup> has one hole in the degenerated orbital pair at  $D_{6h}$  symmetry). After that, the PE as a function of reaction time is oscillating with a period of about 0.1 ps. As seen in PE, both the valley and peak appear on the PE curve at each 0.1 ps (indicated by the arrows in Figure 4A). Superimposed on the large-amplitude oscillations are higher frequency



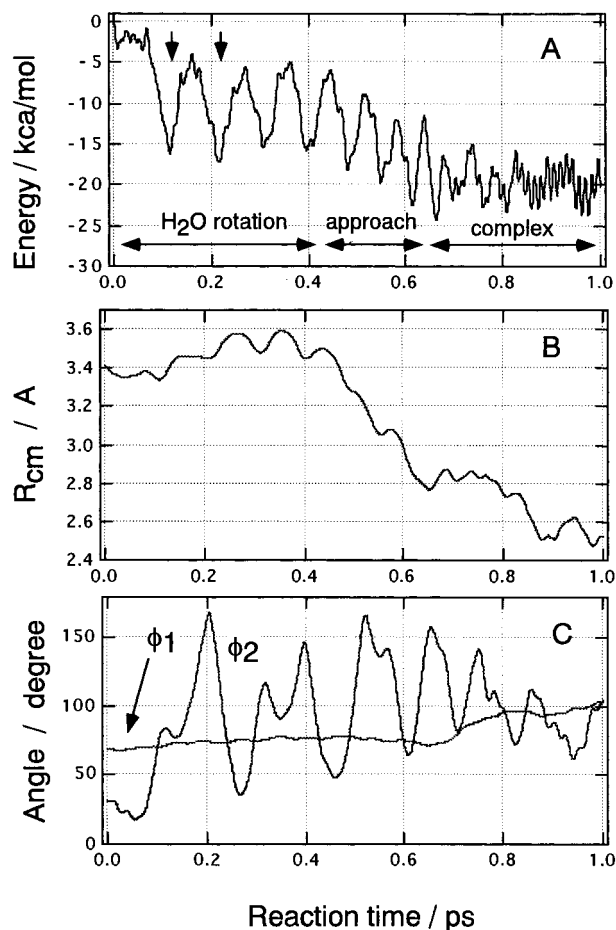


**Figure 4.** Sample trajectory for the  $\text{BzH}_2\text{O}^+$  formed by the vertical ionization of  $\text{BzH}_2\text{O}$  from the equilibrium point: (A) potential energy of the reaction system and (B) intermolecular distance  $R_{\text{cm}}$  and (C) angles ( $\phi_1$  and  $\phi_2$ ) vs. time. Snapshot of the trajectory is given in Figure 5.

oscillations of smaller amplitude. The angles of the hydrogens of  $\text{H}_2\text{O}$  relative to the benzene ring were also plotted as a function of time (Figure 4C), where  $\phi_1$  and  $\phi_2$  are the angles of  $\text{CM}-\text{C}_1-\text{O}$  and  $\text{C}_1-\text{O}-\text{H}$ , respectively (see Figure 1). As seen in parts A and C of Figure 4, the larger-amplitude oscillations in the PE have the same period as the rotation of  $\text{H}_2\text{O}$ . In addition, it was seen from snapshots of the geometry that the PE is minimized when the oxygen of  $\text{H}_2\text{O}$  points toward the benzene ring; i.e., the oxygen orientation forms  $\text{Bz}^+\cdots\text{OH}_2$ . This structure appears at each 0.1 ps owing to the rotation of  $\text{H}_2\text{O}$  above  $\text{Bz}^+$ . It corresponds to the valley in the PE curve. The origin of the fine structure appearing on each peak will be discussed in following paragraph.

As a whole, the PE decreases gradually with increasing reaction time. As clearly seen in Figure 4A, the reaction dynamics following the ionization of  $\text{BzH}_2\text{O}$  is separable into three stages. These stages may be called "H<sub>2</sub>O rotation", "H<sub>2</sub>O approaching", and "complex formation". At time zero, the interaction between Bz and  $\text{H}_2\text{O}$  is suddenly changed by the photoionization from attraction to repulsion on the PES of  $\text{BzH}_2\text{O}^+$ . This is due to the fact that  $\text{Bz}^+\cdots\text{H}_2\text{O}$ , i.e., the configuration with the H atoms arranged on the plane of the ring, is energetically above the dissociation limit ( $\text{Bz}^+ + \text{H}_2\text{O}$ ) on the cation PES, whereas the configuration  $\text{Bz}^+\cdots\text{OH}_2$  is below the dissociation limit. Therefore, in the first stage of the reaction dynamics (0–0.40 ps), the  $\text{H}_2\text{O}$  molecule rotates and moves somewhat away from the benzene ring. After 0.40 ps, the attractive force between  $\text{H}_2\text{O}$  and  $\text{Bz}^+$  becomes larger

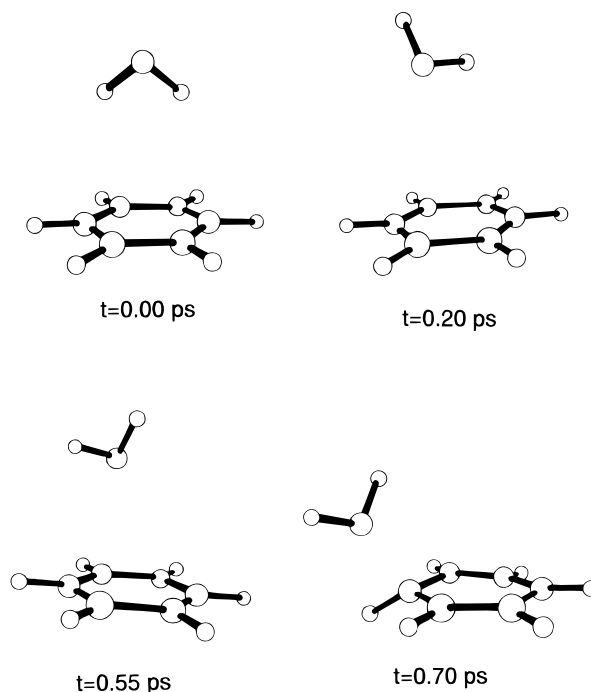


**Figure 5.** Snapshots for the  $\text{BzH}_2\text{O}^+$  ionized from the equilibrium point of  $\text{BzH}_2\text{O}$ .

than the repulsive force so that the  $\text{H}_2\text{O}$  molecule gradually approaches the benzene ring. This approach of  $\text{H}_2\text{O}$  is the second stage. At 0.60 ps, the distance  $R_{\text{cm}}$  is short enough to form the complex. In the third stage (0.65–1.00 ps), the rotation of  $\text{H}_2\text{O}$  is quenched by formation of the  $\text{Bz}^+\cdots\text{H}_2\text{O}$  complex. Thus, the reaction is completed at the third stage. This, then, is an example of a trajectory that results in complex formation rather than dissociation.

Snapshots of the configurations of  $\text{Bz}^+$  and  $\text{H}_2\text{O}$  following the vertical ionization are illustrated in Figure 5. At time zero, the complex has the hydrogen orientation structure ( $\text{Bz}^+\cdots\text{H}_2\text{O}$ ). After 0.2 ps, the water molecule is rotated because of the repulsive (attractive) interactions of the hydrogen (oxygen) with the ring. At 0.55 ps, the water molecule is approaching the ring. At 0.70 ps, the oxygen of  $\text{H}_2\text{O}$  coordinates to one of the carbon atoms by a weak  $\sigma$ -interaction. At 1.0 ps (figure is not given), the complex is completely formed. The available energy of the complex becomes distributed in the vibrational modes of  $\text{BzH}_2\text{O}^+$  complex.

As mentioned above, the PE for  $\text{BzH}_2\text{O}^+$  varied significantly as a function of time, and each peak of the PE has fine structure. To elucidate the origin of this fine structure, a trajectory of free benzene after ionization was calculated in the same manner. The result for the ionization of benzene is given in Figure 6. At time zero, the benzene cation has  $D_{6h}$  symmetry and equal C–C bond distances ( $r_1 = r_2 = 1.38 \text{ \AA}$ ). The benzene ring is deformed after the ionization, and the C–C bonds alternate in lengths. We denote the greater lengths by  $r_1$  and the lesser lengths by  $r_2$ . The time dependence of the distances is shown in Figure 6B. After ionization, immediately,  $r_1$  is rapidly elongated to  $1.50 \text{ \AA}$  whereas  $r_2$  is shortened to  $1.35 \text{ \AA}$ . The periodic variation of PE is caused by the mutual oscillation between  $r_1$  and  $r_2$ . The period of these oscillations is roughly 0.08 ps. This result strongly indicates that the fine structure appearing in the PE curve is due to the periodic deformation of benzene ring after the ionization.

*Trajectories from the Classical Turning Points in the Franck–Condon Region.* The trajectory started from the outer

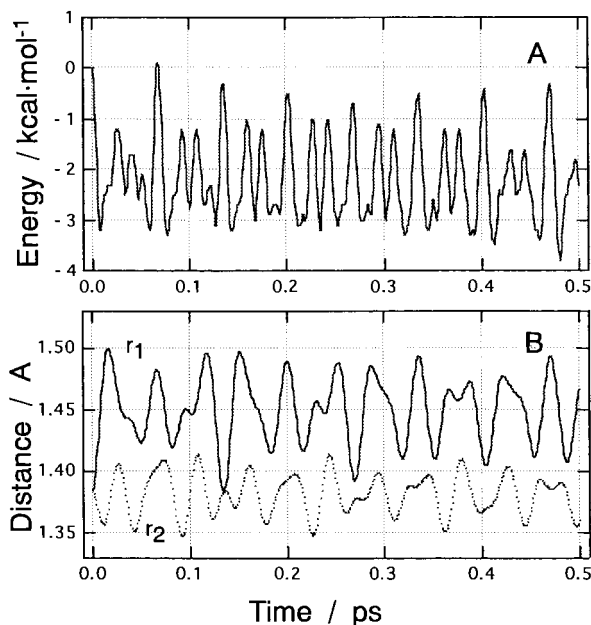


**Figure 6.** Sample trajectory for free benzene cation ( $Bz^+$ ) formed by the vertical ionization of Bz: (A) potential energy and (B) interatomic distances  $r_1$  and  $r_2$  vs time.

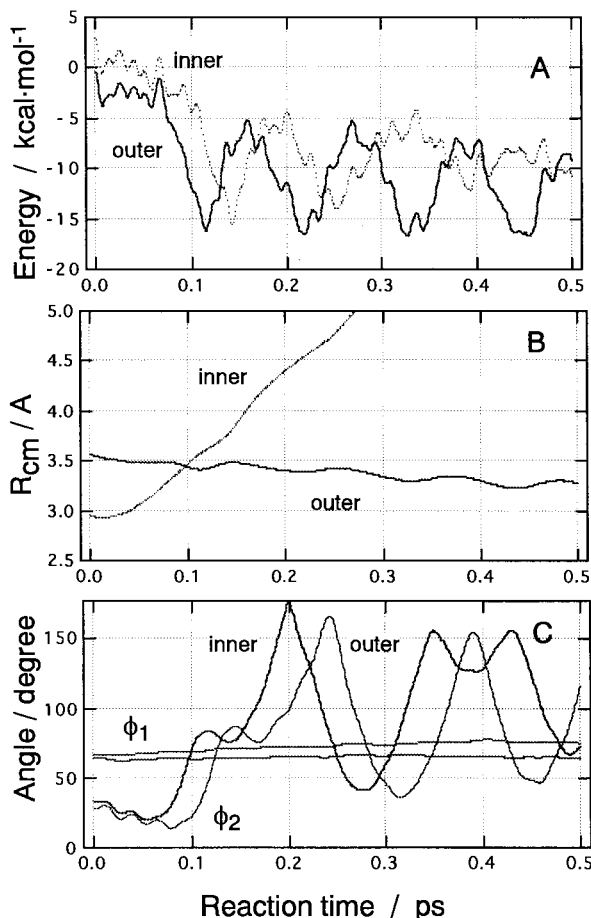


**Figure 7.** Trajectories for the  $BzH_2O^+$  formed from the inner and outer classical turning points in the Franck-Condon region: (A) the potential energy of the reaction system and (B) intermolecular distance  $R_{cm}$  and (C) angle vs time.

turning point in the FC region is summarized by the solid lines in Figure 7. The zero of potential energy (PE) is the same as in Figure 4. The energy at time zero is slightly lower than the zero energy level because the vertical transition from the outer

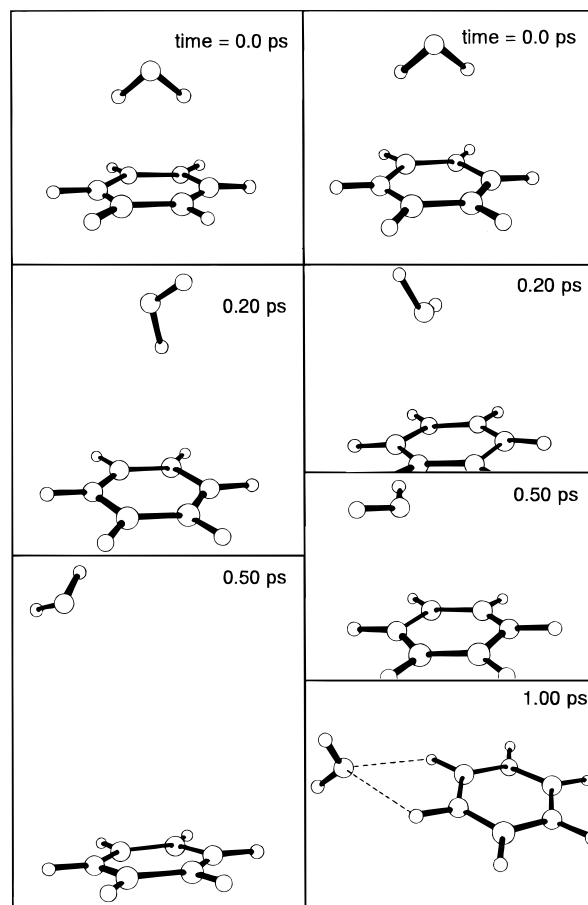


**Figure 8.** Snapshots for the  $BzH_2O^+$  ionized from the inner (left) and outer (right) classical turning points in the Franck-Condon region.

turning point brings the system to a point on the  $BzH_2O^+$  surface that is slightly lower in energy than the point reached from the equilibrium position on the neutral surface. The trajectory from the outer turning point is quite similar to that from the equilibrium point. This trajectory leads to complex formation. The PE curve is also similar to that from the optimized point; the fine structure caused by the deformation of the benzene ring and the valley and peak caused by H<sub>2</sub>O rotation are features of the PE curve. As shown in Figure 7B, the distance of  $R_{cm}$  decreases gradually with increasing reaction time, indicating that the H<sub>2</sub>O molecule approaches the benzene ring after the ionization. The complex is completely formed at 1.0 ps.

The trajectory started from the inner classical turning point is summarized by the dashed lines in Figure 7. The energy at time zero is 5.0 kcal/mol higher than that of the equilibrium point. The reaction started from the inner turning point is much different from those from both equilibrium and the outer turning points;  $R_{cm}$  increases strongly with increasing reaction time as shown in Figure 7B, indicating that the H<sub>2</sub>O molecule immediately escapes from the benzene ring after the ionization. The trajectory from the inner turning point leads to the dissociation products  $Bz^+$  and H<sub>2</sub>O. The PE curve shows oscillations that are indicative of H<sub>2</sub>O rotation (Figure 7, dotted line). However, the valley becomes shallower as reaction time increases. This is expected, since the interaction between H<sub>2</sub>O and  $Bz^+$  decreases with increasing  $R_{cm}$ . At times longer than 0.5 ps, the PE approaches its asymptotic value.

Snapshots of the structures following the vertical ionization are illustrated in Figure 8. Right and left parts of the figure represent the snapshots for trajectories started from outer and inner classical turning points, respectively. Note that the

**TABLE 3: Summary of Trajectory Calculations Started from Several Points in the Franck–Condon Region**

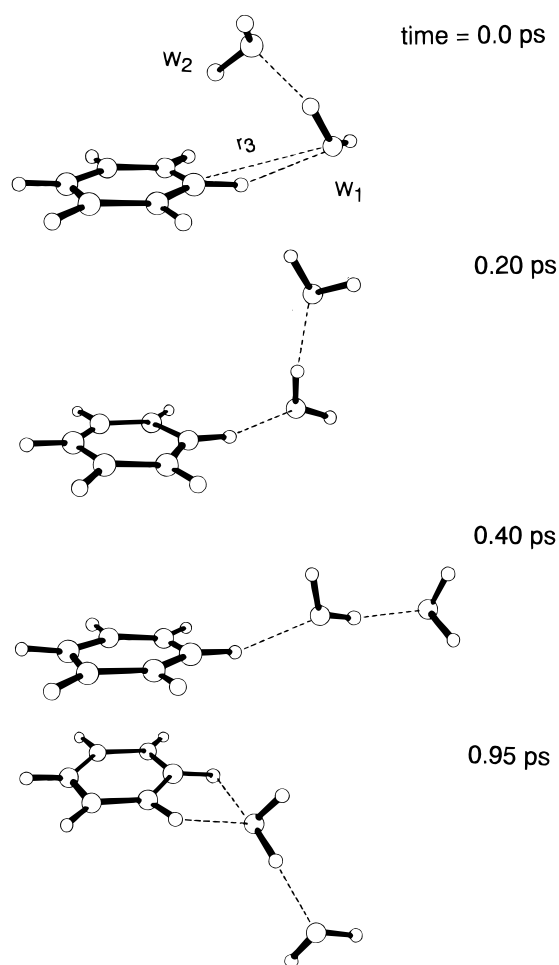
$R_{cm}/\text{\AA}$	product channel	comment
2.9500	dissociation	inner classical turning point
3.3721	dissociation	
3.3867	dissociation	
3.3901	dissociation	
3.3950	complex	optimized point
3.4133	dissociation	
3.4384	complex	
3.4672	complex	
3.5191	complex	
3.5214	complex	
3.6000	complex	outer classical turning point

difference in the trajectories is only  $R_{cm}$  ( $R_{cm} = 3.60$  and  $2.95$  Å, respectively). At time zero, the complex has the hydrogens pointed toward the ring in both complexes. After 0.20 ps, in the trajectory started from the inner turning point, the  $\text{H}_2\text{O}$  molecule is separating from the benzene ring and the rotation of  $\text{H}_2\text{O}$  is highly enhanced by the strong repulsive surface. After 0.50 ps,  $\text{H}_2\text{O}$  is fully separated from  $\text{Bz}^+$  and the interaction between  $\text{H}_2\text{O}$  and the benzene ring becomes negligibly small. In contrast, in the trajectory started from the outer turning point, the  $\text{H}_2\text{O}$  molecule is somewhat close to  $\text{Bz}^+$  at 0.20 ps. The rotation of the  $\text{H}_2\text{O}$  molecule is enhanced by the repulsive interaction as in the case of the trajectory from the inner turning point. At 0.50 ps, the oxygen of  $\text{H}_2\text{O}$  has a slow approach to the plane of the ring. At 1.0 ps, complex formation is essentially complete.

*Trajectories from Several Points in FC Region.* In addition to the three above-mentioned trajectories, eight additional starting points in the FC region were examined in the trajectory calculations. These points were randomly chosen points on the trajectory for the  $\text{BzH}_2\text{O}$  neutral complex (Figure 3). The results of the trajectory calculations from the selected points are summarized in Table 3 together with those of the three specific points. As clearly seen in Table 3, the reaction channel is mainly determined by the location of ionization points in the FC region; the dissociation channel is open in the case of shorter  $R_{cm}$ , whereas the complex formation channel is associated by the ionization at longer  $R_{cm}$ . The channels are roughly mixed in the medium region of  $R_{cm}$ . The present study indicates that the location of the ionization point in the FC region has a considerable effect on the relative accessibility of the product channels.

*C. Ionization Process in  $\text{Bz}(\text{H}_2\text{O})_2$ .* The number of solvent molecules would be a dominant factor in photoionization dynamics of  $\text{Bz}(\text{H}_2\text{O})_n$  clusters. To elucidate the solvent effect on the dynamics in more detail, a preliminary trajectory calculation of  $\text{Bz}(\text{H}_2\text{O})_2$  was carried out in the same manner. We chose only an optimized structure of  $\text{Bz}(\text{H}_2\text{O})_2$  as the starting point of the ionization. The optimized structure of  $\text{Bz}(\text{H}_2\text{O})_2$  is illustrated in Figure 9 (0.0 ps). This optimized structure is the one obtained by Sorenson et al.<sup>13</sup> One of the water molecules ( $W_1$ ) is hydrogen-bonded to the C–H hydrogen of the benzene ring, and the other water molecule ( $W_2$ ) is hydrogen-bonded to  $W_1$  and is located such that it interacts weakly with  $\text{Bz}$ .

The single trajectory that was run is summarized in Figures 9 and 10. Initially, molecule  $W_2$  moves rapidly from the ring because of the repulsive interaction between  $\text{Bz}^+$  and  $W_2$ . However, the  $W_2$  molecule does not dissociate from the system, but rather it remains hydrogen-bonded to  $W_1$ . As shown in Figure 10B, the distance between the oxygens ( $r_{OO}$ ) as a function of time is highly oscillating, but the hydrogen bond was not

**Figure 9.** Snapshots for the  $\text{Bz}(\text{H}_2\text{O})_2^+$  ionized from the equilibrium point of  $\text{Bz}(\text{H}_2\text{O})_2$ .

broken in this trajectory. At 0.95 ps,  $W_1$  is still bonded to  $\text{Bz}^+$ . The final product is a  $\text{Bz}(\text{H}_2\text{O})_2^+$  cluster.

#### 4. Discussion

**Model of the Photodissociation of  $\text{BzH}_2\text{O}$ .** In this study, we investigated the ionization processes of the  $\text{BzH}_2\text{O}$  complex by means of direct ab initio dynamics calculations. On the basis of the present results, we propose a reaction model for the ionization process of  $\text{BzH}_2\text{O}$ . Potential energy curves expressed for  $\text{BzH}_2\text{O}$  and  $\text{BzH}_2\text{O}^+$  are schematically illustrated in Figure 11. The lower curve (curve a) represents the potential energy along the dissociation coordinate for the  $\text{BzH}_2\text{O}$  neutral complex. The configuration of the complex is constrained to the dipole orientation form ( $\text{Bz}\cdots\text{H}_2\text{O}$ ). The Franck–Condon (FC) region encompasses a wide range of  $R_{cm}$  because of the fact that the PEC is very shallow. In other words, vertical ionization produces  $\text{BzH}_2\text{O}^+$  in a wide range of configurations.

The corresponding curve for the cationic system ( $\text{Bz}^+\cdots\text{H}_2\text{O}$ ) is given by an upper curve (curve b). In this curve the nuclei are constrained as for  $\text{BzH}_2\text{O}$ , i.e., in the dipole orientation form. The FC region for the ionization of  $\text{BzH}_2\text{O}$  is illustrated by the hatched region. It should be noted that curve b is always repulsive and has negative gradients of PE in the FC region. On the other hand, curve c, which is calculated by constraining the structure to the oxygen orientation form, has a considerable attractive portion and is significantly lower than curve b. In other words, the potential energy of the cluster ion is very much dependent on the orientation of the  $\text{H}_2\text{O}$  molecule.

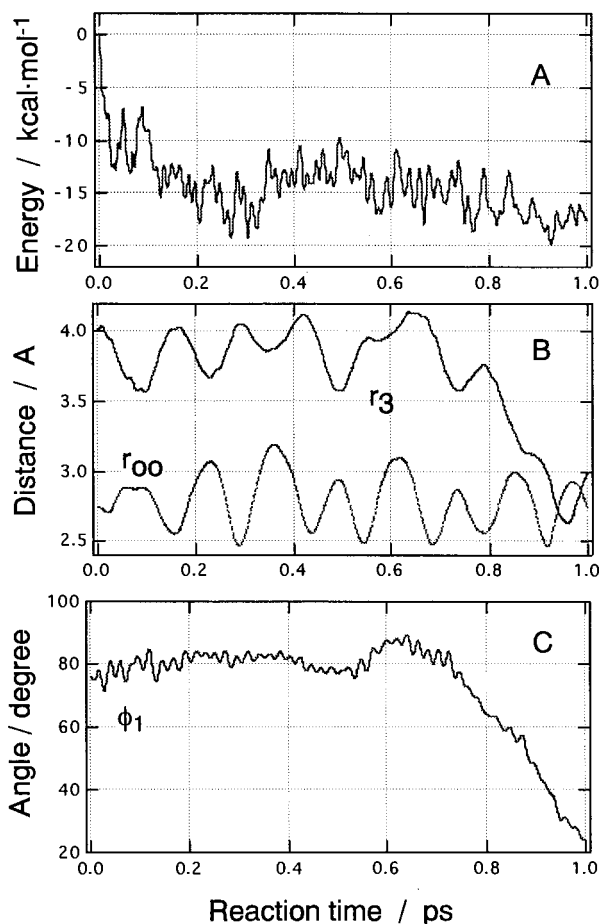


**Figure 10.** Trajectories for the  $Bz(H_2O)_2^+$  formed from the equilibrium point: (A) the potential energy of the reaction system and (B) distances  $r_{00}$ ,  $r_3$ , and  $R_{cm}$  and (C) angle ( $\phi_1$ ) vs time.

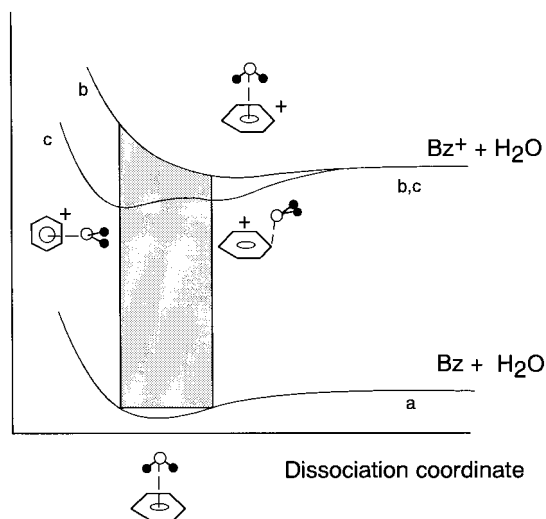


**Figure 11.** Reaction model for the photoionization process of  $BzH_2O$ . Lower (a) and upper (b, c) curves are potential energies for neutral and ionic species, respectively.

Because of the specific feature of PESs as above-mentioned, it is theoretically predicted that there are two product channels in the photoionization of  $BzH_2O$ : a dissociation channel and a rearrangement channel. The photoionization from the inner FC region leads to the dissociation channel because of the fact that the transition point on curve b is strongly repulsive. The  $H_2O$  dissociates rapidly from the benzene ring ( $Bz^+$ ). This dissociation is complete within 0.5–1.0 ps. On the other hand, the

photoionization from the outer FC region leads to a long-lived complex  $Bz^+ \cdots OH_2$ . The lifetime of the complex is at least longer than 2.0 ps. The reaction from the middle FC region (i.e., around the equilibrium point of  $BzH_2O$ ) will give both channels (may produce either rearrangement  $BzH_2O^+$  or  $Bz^+ + H_2O$ ). Recently, Cheng et al. observed that the photoionization of  $BzH_2O$  leads to two reaction channels: dissociation and complex formation.<sup>6</sup> The present calculation agrees with their experimental results. The binding energy of  $Bz^+ \cdots H_2O$  estimated from their experiment data (4 kcal mol<sup>-1</sup>) is, however, significantly smaller than the results of our theoretical calculation (13 kcal mol<sup>-1</sup>). This underestimate of the binding energy in the experiment may be due to the complexity of the PES for  $BzH_2O^+$ . Very recently, Courty et al. showed, on the basis of their experiment and a semiempirical calculation, that the binding energy of  $Bz^+ \cdots H_2O$  is 9.22 kcal mol<sup>-1</sup>, which is much closer to the results of the present calculation.<sup>14</sup>

### Concluding Remarks

We have introduced several approximations in calculating the potential energy surface and in treating the reaction dynamics. First, we assumed that  $BzH_2O^+$  has no excess energy at the initial step of the trajectory calculation (time = 0.0 ps). In addition, the momentum vectors (velocities) of atoms were assumed to be zero because of very low temperature (10 K). These assumptions may cause a slight change of lifetime and energy distribution of the  $BzH_2O^+$  complex. In the case of higher excess energy, the dissociation into  $Bz^+$  and  $H_2O$  may occur more efficiently in the  $BzH_2O^+$  complex. Moreover, in the case of the  $Bz(H_2O)_2^+$  complex,  $H_2O$  may dissociate easily from the  $BzH_2O^+$  complex. This effect was not considered in the present calculations. It should be noted, therefore, that the present model is limited in the case of no excess energy.

Second, we assumed an HF/3-21G multidimensional potential energy surface in the trajectory calculations throughout. This level of theory is probably adequate for the qualitative treatment of the photoionization dynamics of  $BzH_2O$ , which has been the subject of the present paper. However, a more accurate PES is probably necessary for a reliable qualitative treatment (for example, of the branching ratio of the product channels). Despite the several assumptions introduced here, the results enable us to obtain valuable information on the mechanism of the photoionization process in the  $Bz(H_2O)_n$  cluster ( $n = 1$  and 2).

**Acknowledgment.** The author is indebted to the Computer Center at the Institute for Molecular Science (IMS) for the use of the computing facilities. The author acknowledges partial support from a Grant-in-Aid from the Ministry of Education, Science, Sports and Culture of Japan.

### References and Notes

- (1) Müller-Dethlefs, K.; Dopfer, O.; Wright, T. G. *Chem. Rev.* **1994**, *94*, 1845.
- (2) Gonohe, N.; Abe, H.; Mikami, N.; Ito, M. *J. Phys. Chem.* **1985**, *89*, 3462.
- (3) (a) Zwier, T. S. *Annu. Rev. Phys. Chem.* **1996**, *47*, 205 and references therein. (b) Gotch, A. J.; Zwier, T. S. *J. Chem. Phys.* **1992**, *96*, 3388.
- (4) Courty, A.; Mons, M.; Calve, J. Le; Piuze, F.; Dimicoli, I. *J. Phys. Chem. A.* **1997**, *101*, 1145.
- (5) (a) Kim, K. S.; Lee, J. Y.; Soon, H.; Kim, J.; Jang, J. H. *Chem. Phys. Lett.* **1997**, *265*, 497. (b) Augspurger, J. D.; Dyksta, C. E.; Zwier, T. S. *J. Phys. Chem.* **1992**, *96*, 7252; **1993**, *97*, 980. (c) Linse, P. *J. Comput. Chem.* **1998**, *9*, 505. (d) Gregory, J. K.; Clary, D. C. *Mol. Phys.* **1996**, *88*, 33.



- (6) Cheng, B.-M.; Grover, J. R.; Walters, E. A. *Chem. Phys. Lett.* **1995**, 232, 364.
- (7) (a) Tachikawa, H. *J. Chem. Phys.* **1998**, 108, 3966. (b) Tachikawa, H.; Ohnishi, K.; Hamabayashi, S.; Yoshida, H. *J. Phys. Chem. A* **1997**, 101, 2229. (c) Tachikawa, H. *J. Phys. Chem.* **1995**, 99, 225. (d) Abe, M.; Inagaki, Y.; Springsteen, L. L.; Matsumi, Y.; Kawasaki, M.; Tachikawa, H. *J. Phys. Chem.* **1994**, 98, 12641. (e) Tachikawa, H.; Hamabayashi, T.; Yoshida, H. *J. Phys. Chem.* **1995**, 99, 16630. (f) Tachikawa, H.; Takamura, H.; Yoshida, H. *J. Phys. Chem.* **1994**, 98, 5298. (g) Tachikawa, H.; Ohtake, A.; Yoshida, H., *J. Phys. Chem.* **1993**, 97, 11944.
- (8) (a) Tachikawa, H. *J. Phys. Chem. A* **1997**, 101, 7475. (b) Tachikawa, H. *J. Phys. Chem.* **1996**, 100, 17090. (c) Tachikawa, H.; Kumaguchi, K. *Int. J. Mass Spectrom. Ion Processes* **1997**, 164, 39. (d) Program code of the direct ab initio dynamics calculation was created by our group.
- (9) Ab initio MO calculation program. Frisch, M. J.; Trucks, G. W.; Schlegel, H. B.; Gill, P. M. W.; Johnson, B. G.; Robb, M. A.; Cheeseman, J. R.; Keith, T.; Petersson, G. A.; Montgomery, J. A.; Raghavachari, K.; Al-Laham, M. A.; Zakrzewski, V. G.; Ortiz, J. V.; Foresman, J. B.; Cioslowski, J.; Stefanov, B. B.; Nanayakkara, A.; Challacombe, M.; Peng, C. Y.; Ayala, P. Y.; Chen, W.; Wong, M. W.; Andres, J. L.; Replogle, E. S.; Gomperts, R.; Martin, R. L.; Fox, D. J.; Binkley, J. S.; Defrees, D. J.; Baker, J.; Stewart, J. P.; Head-Gordon, M.; Gonzalez, C.; Pople, J. A.: *Gaussian 94*, revision D.3; Gaussian, Inc.: Pittsburgh, PA, 1995.
- (10) Pribble, R. N.; Zwier, T. S. *Science* **1994**, 265, 75.
- (11) Gutowsky, H. S.; Emilsson, T.; Arunan, E. *J. Chem. Phys.* **1993**, 99, 4883.
- (12) Suzuki, S.; Green, P. G.; Bumgarner, R. E.; Dasgupta, S.; Goddard, Ö. W. A.; Blake, G. A. *Science* **1992**, 257, 942.
- (13) Sorenson, J. M.; Gregory, J. K.; Clary, D. C. *J. Chem. Phys.* **1997**, 106, 849.
- (14) Courty, A.; Mons, M.; Dimicoli, I.; Piuze, F.; Gaigeot, M. P.; Brenner, V.; de Pujo, P.; Millie, P. *J. Phys. Chem. A* **1998**, 102, 6590.